NUMERICAL CALCULATION OF LAMINAR COMPRESSIBLE BOUNDARY LAYERS IN UNSTEADY FLOW

J. Piquet

Translation of: "Calcul numérique de couches limites laminaires compressibles en régime instationnaire," Journal de Mecanique, Vol. 11, No. 1, March, 1972, pp. 5 - 27.

NATIONAL AERONAUTICS AND SPACE ADMINISTRATION
WASHINGTON, D. C. 20546 AUGUST 1972

23p

NUMERICAL CALCULATION OF LAMINAR COMPRESSIBLE BOUNDARY LAYERS IN UNSTEADY FLOW

Jean Piquet[1]

ABSTRACT. Calculations of some velocity and temperature boundary layers on a flat plate, especially behind a shock, have been carried out. Such boundary layers have the following structure: two quasi-stationary flows, corresponding to known analytical solutions expressed in terms of similarity variables, merge in an interaction region. The governing equations in this region are singular-parabolic and admit boundary conditions generally associated with elliptic equations. These equations are solved successfully by a difference scheme converging in a suitable way.

1. INTRODUCTION

/5*

This paper discusses certain velocity and temperature boundary layers on a flat plate. A similarity hypothesis takes the place of knowledge of an initial condition at x = 0. Three problems are treated in this way, after being formulated in Crocco's system of variables and functions. Problem A concerns an impulsively started flat plate in incompressible flow; problem B, the compressible boundary /6 layer induced by shock; problem C, the shock tube.

---

[1]ONERA, 29, avenue de la Division-Leclerc, 92-Chatillon-sous-Bagneux, France.

*Numbers in the margin indicate pagination in the original foreign text.

The boundary layer is composed of three regions, in each of which a system of partial differential equations must be solved. Outside one region, the interaction zone, the equations governing the phenomena reduce, after analytic transformations which allow the separation of variables, to simple ordinary differential equations, treated numerically by an implicit scheme after they are made unsteady.

In the interaction zone, the equations are singular and parabolic, and have elliptic boundary conditions which involve solutions previously calculated in the other regions. After making them unsteady, use of an explicit unconditionally stable scheme allows termination of the numerical solution of the problems treated.

2. GENERAL EQUATIONS

Before any analysis, the equations are written in an appropriate dimensionless form. The reference values, noted below with an index $_0$, are in general experimental conditions of the study. L_0 is a characteristic length of the body studied; Q_0, a reference velocity which measures, in a boundary-layer problem, the magnitude of the velocity $\overline{U}$ at the edge of the boundary layer. In addition, the reference temperature and pressure are not independent, and are given by the expressions

$$\left| T_0 = \frac{Q_0^2}{\bar{c}_p - \bar{c}_v} \right| \quad \text{and} \quad \left| p_0 = \rho_0 Q_0^2, \right| \tag{1}$$

where the specific heats at constant pressure and at constant volume ($\overline{c}_p$ and $\overline{c}_v$, respectively) are assumed constant. The dimensionless quantities are obtained from the dimensioned quantities (overlined) by

$$\left| \begin{array}{lll} y = \bar{y}\sqrt{\frac{\rho_0}{\mu_0 t_0}}, & t = \frac{\bar{t}}{t_0}, & x = \frac{\bar{x}}{L_0}, \\ u = \frac{\bar{u}}{Q_0}, & U = \frac{\bar{U}}{Q_0}, & v = \bar{v}\sqrt{\frac{\rho_0 t_0}{\mu_0}}, \\ c_p = \frac{\bar{c}_p}{\bar{c}_p - \bar{c}_v}, & p = \frac{\bar{p}}{\rho_0 Q_0^2}, & T = \frac{(\bar{c}_p - \bar{c}_v)\bar{T}}{Q_0^2}, \end{array} \right| \tag{2}$$

where μ_0, ρ_0, $t_0 = L_0 Q_0^{-1}$ represent viscosity, density, and reference time, respectively.

The Reynolds number of the flow, $\left| Re = \frac{\rho_0 Q_0 L_0}{\mu_0} \right|$, does not appear in the equations, /7 which in the unsteady laminar compressible case take the following form:

$$\left\{\begin{array}{c} \rho(u_{,t}+uu_{,x}+vu_{,y})=-p_{,x}+(\mu u_{,y})_{,y}, \\ \rho_{,t}+u\rho_{,x}+v\rho_{,y}=-\rho\frac{r_{,x}}{r}u-\rho(u_{,x}+v_{,y}), \\ \rho c_p(\mathrm{T}_{,t}+u\mathrm{T}_{,x}+v\mathrm{T}_{,y})=p_{,t}+up_{,x}+\left(\frac{\mu c_p}{\mathrm{Pr}}\mathrm{T}_{,y}\right)_{,y}+\mu u_{,y}^2. \end{array}\right| \tag{3}$$

It is necessary to add the two thermodynamic laws:

$$\left\{\begin{array}{l} p=\rho\mathrm{T}, \\ \mu=\chi\mathrm{T}^{\omega}, \end{array}\right| \tag{4}$$

the boundary conditions:

$$\left\{\begin{array}{llll} y=0, & \mathrm{T}=\mathrm{T}_w(x,t); & u=0; & v=v_s(x,t), \\ y=\infty, & \mathrm{T}=\mathrm{T}_e(x,t); & u=\mathrm{U}(x,t) & \end{array}\right| \tag{5}$$

and the initial conditions:

$$\left\{\begin{array}{llll} x=x_0, & u=u_1(t,y); & \mathrm{T}=\mathrm{T}_1(t,y), & \\ t=t_0, & u=u_0(x,y); & \mathrm{T}=\mathrm{T}_0(x,y) & \end{array}\right| \tag{6}$$

for the problem to be properly stated.

The symbol $\underline{u}_{,t}$ indicates the partial derivative of the function u with respect to the variable t. The Prandtl number Pr will be assumed constant, as will the coefficients χ and ω which appear in the viscosity law.

In addition, the functions T_w, T_e, $\underline{v}_s$ (velocity of blowing at the wall), u_1, u_0, T_1 and T_0 are assumed to be known, as well as r (equal to 1 for a plane problem, or a function of x for an axisymmetric problem) and p(x,t) which, in any boundary-layer problem, are given. In particular:

$$\left\{\begin{array}{l} -p_{,x}=\rho_e(\mathrm{U}_{,t}+\mathrm{U}\mathrm{U}_{,t}), \\ p_{,t}=\rho_e c_p(\mathrm{T}_{e,t}+\mathrm{U}\mathrm{T}_{e,x})+\mathrm{U}(\mathrm{U}_{,t}+\mathrm{U}\mathrm{U}_{,x}), \end{array}\right| \tag{7}$$

where the quantities with the index e represent given values outside the boundary layer.

In general, knowledge of the exterior flow U(t,x) is a difficult problem in itself. This is why a first approach to the compressible problem consists of limiting oneself to the case of flow over a flat plate: /8

$$p_{,x}=0; \quad p_{,t}=\rho_e c_p(\mathrm{T}_{e,t}+\mathrm{U}\mathrm{T}_{e,x}) \tag{8}$$

(2) The geometry of the problem requires, moreover, that $\mathrm{T}_{e,x}$ = 0 almost everywhere, contact discontinuities being tolerated in the exterior flow.

The numerical solution of various problems belonging to the compressible case can thus be carried out — in particular, the coupling of velocity and temperature, and the effect of the Prandtl number.

3. FORMULATION OF THE PROBLEM

The group of equations (3) through (7) is treated after the Crocco transformation, assuming that (8) holds. Choice of variables t, x, $\eta = \frac{u}{U}$ and of unknown functions T, $\varphi = \frac{\mu u_{,y}}{U}$ leads to

$$\left\{ \begin{array}{l} \dfrac{\varphi^2 \varphi_{,\eta\eta}}{\rho\mu} - \varphi_{,t} - \eta\varphi_{,x} + \dfrac{\varphi}{\rho\mu}\left[(\rho\mu)_{,t} + \eta(\rho\mu)_{,x}\right] = 0, \\ \dfrac{\varphi^2 T_{,\eta\eta}}{\rho\mu} - T_{,t} - \eta T_{,x} + D + \dfrac{\varphi^2}{\rho\mu c_p} + \dfrac{\varphi\varphi_{,\eta} T_{,\eta}}{\rho\mu}\left(\dfrac{1 - Pr}{Pr}\right) = 0, \end{array} \right. \tag{9}$$

where $D = \frac{\rho_e}{\rho c_p}$.

System (9) has the following boundary conditions:

$$\left\{ \begin{array}{ll} \varphi_{,\eta} = \rho v_s & \text{and} \quad T = T_w \quad \text{at} \quad \eta = 0, \\ \varphi = 0 & \text{and} \quad T = T_e \quad \text{at} \quad \eta = 1. \end{array} \right. \tag{10}$$

Taking into account (4), the problem is properly stated when $\phi(x = x_0)$, $T(x = x_0)$, $\phi(t = t_0)$, $T(t = t_0)$ are specified. Unfortunately, the velocity profiles at $x = x_0$, for example, are unknown for the flat plate; therefore, the method used in reference [1] is inapplicable to the present case.

This difficulty can be avoided by noting that system (9) remains invariant under the transformation

$$\left\{ \begin{array}{l} t \to kt; \quad x \to kx; \quad \eta \to \eta; \\ \varphi \to \dfrac{\varphi}{\sqrt{k}}; \quad T \to T; \quad \rho\mu \to \rho\mu; \quad p \to p. \end{array} \right. \tag{11}$$

If one limits oneself to the case $v_s = 0$, T_e and T_w constant, the boundary conditions (10) are also invariant.

Then, taking $\xi = \frac{x}{t}$ and η as independent variables, relation (11) shows that the unknown functions have the forms

$$\varphi(t, x, \eta) = \frac{\Phi(\xi, \eta)}{\sqrt{x}}; \qquad T = T(\xi, \eta); \qquad v(t, x, \eta) = \frac{V(\xi, \eta)}{\sqrt{x}} \tag{12}$$

which leads to the system of equations /9

$$\frac{\Phi^2\Phi_{,\eta\eta}}{\rho\mu} - \xi(\eta-\xi)\Phi_{,\xi} + \frac{\eta\Phi}{2} + \frac{\Phi}{\rho\mu}\xi(\eta-\xi)[\rho\mu]_{,\xi} = 0; \tag{13a}$$

$$\frac{\Phi^2 T_{,\eta\eta}}{\rho\mu} - \xi(\eta-\xi)T_{,\xi} + \xi\frac{\rho_e}{\rho}(1-\xi)T_{e,\xi} + \frac{\Phi^2}{\rho\mu c_p} + \frac{\Phi\Phi_{,\eta}T_{,\eta}}{\rho\mu}\left(\frac{1-\mathrm{Pr}}{\mathrm{Pr}}\right) = 0; \tag{13b}$$

$$\frac{\Phi}{\mu}[V-(\eta-\xi)V_{,\eta}] = \frac{\Phi\Phi_{,\eta}}{\rho\mu} - (\eta-\xi)\left[\frac{\Phi}{p\mu\,\mathrm{Pr}}(\Phi T_{,\eta})_{,\eta} + \frac{\Phi^2}{p\mu c_p} - \xi c_p(1-\xi)\frac{T_{e,\xi}}{T_e}\right] = 0. \tag{13c}$$

It should be noted that the choice of $\xi = \frac{t}{x}$ and η as independent variables, which is strictly equivalent, leads to the form

$$\varphi(t, x, \eta) = \frac{\Psi(\xi, \eta)}{\sqrt{t}}; \qquad T = T(\xi, \eta); \qquad v(t, x, \eta) = \frac{W(\xi, \eta)}{\sqrt{t}} \tag{14}$$

and to the equations

$$\begin{cases} \dfrac{\Psi^2\Psi_{,\eta\eta}}{\rho\mu} - (\eta-\xi)\Psi_{,\xi} + \dfrac{\Psi}{2} + \dfrac{\Psi}{\rho\mu}(\eta-\xi)[\rho\mu]_{,\xi} = 0, \\ \dfrac{\Psi^2 T_{,\eta\eta}}{\rho\mu} - (\eta-\xi)T_{,\xi} + \dfrac{\rho_e}{\rho}(1-\xi)T_{e,\xi} + \dfrac{\Psi^2}{\rho\mu c_p} + \dfrac{\Psi\Psi_{,\eta}T_{,\eta}}{\rho\mu}\left(\dfrac{1-\mathrm{Pr}}{\mathrm{Pr}}\right) = 0, \\ \dfrac{\Psi}{\mu}[W-(\eta-\xi)W_{,\eta}] = \dfrac{\Psi\Psi_{,\eta}}{\rho\mu} - (\eta-\xi)\left[\dfrac{\Psi}{p\mu\,\mathrm{Pr}}(\Psi T_{,\eta})_{,\eta} + \dfrac{\Psi^2}{p\mu c_p} - c_p(1-\xi)\dfrac{T_{e,\xi}}{T_e}\right] = 0. \end{cases} \tag{15}$$

In the following, we shall concern ourselves with system (13), having established once and for all that the course described is followed faithfully in the treatment of system (15). The nature of the problem will allow a choice between the functions Φ and Ψ (though related by $\Phi = \Psi\sqrt{\xi}$), and as a consequence, between systems (13) and (15). To equations (13a) and (13b), it is necessary to add the boundary conditions

$$\begin{cases} \Phi_{,\eta} = 0 & \text{and} \quad T = T_w & \text{at} \quad \eta = 0, \\ \Phi = 0 & \text{and} \quad T = T_e & \text{at} \quad \eta = 1. \end{cases} \tag{16}$$

Note - When the temperature is not given on the wall, one assumes that the heat transfer per unit area per unit time, q_w, is known:

$$q_w = -\frac{\mu c_p}{\mathrm{Pr}}T_{,y}\Big|_{y=0} = -\frac{c_p\varphi}{\mathrm{Pr}}T_{,\eta}\Big|_{\eta=0}. \tag{17}$$

Thus the boundary condition at $\eta = 0$ relates to $T_{,\eta}$ and not to T. It must be pointed out that q_w must have a particular form: invariance under transformation /10 (11) assumes

$$\begin{cases} q_w = \dfrac{Q_w}{\sqrt{x}} & \text{in case (12)} \\ q_w = \dfrac{Q_w}{\sqrt{t}} & \text{in case (14)}, \end{cases} \tag{18}$$

The quantity Q_w is a given constant.

4. PHYSICAL PROBLEMS DISCUSSED

4.1 Boundary Layers on a Semi-Infinite Flat Plate: Problems A and B

The leading edge of a semi-infinite flat plate is the origin of the (x,y) coordinate system, and the plate lies along the positive x axis (axes fixed to the plate). In this case, the characteristic length is the abscissa of the point at which the velocity profile is studied, so that x = 1, and consequently $\xi = t^{-1}$ and $\Phi = \varphi'$.

Problem A - The plate is impulsively started at time t = 0, and carried from velocity U = 0 to velocity U = 1. When the conditions on ξ are defined, equations (13a) and (13b), together with boundary conditions (16), permit solution of the problem. The fluid is, moreover, assumed to be incompressible: i.e., $\rho\mu = 1$ (this problem was not considered in [1]). The validity of the scheme could thus be tested for the simplest case, corresponding to equations (13a) and (13b) decoupled. The results obtained are in good agreement with those of Hall [2] and of Lam and Crocco [3] (see Figure 1).

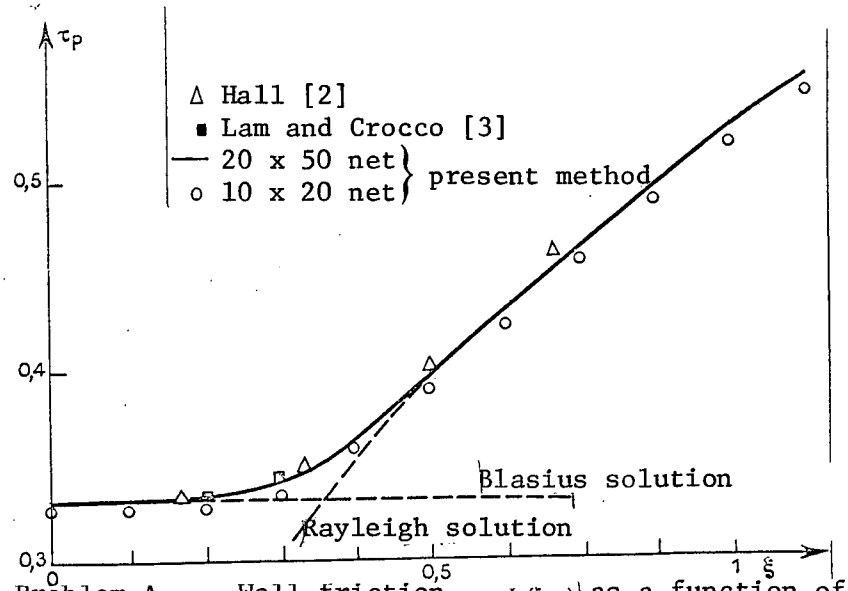

Figure 1. Problem A. Wall friction $\tau_p = \Phi(\xi, 0)$ as a function of $\xi = x/t$.

Problem B - A plane shock moves over a semi-infinite flat plate and induces a boundary layer between the shock and the leading edge of the plate. This problem, which includes Problem A as a special case, has been treated for any Prandtl numbers or viscosity laws. The results given by Lam and Crocco [3] correspond to decoupled temperature and velocity boundary layers, and the numerical method they use diverges.

4.2. Shock-Tube Problem: Problem C

At $t \leq 0$, two chambers at different pressures are separated by a diaphragm located at $x = 0$. The two chambers are at the temperature $\overline{T}_w$ of their wall. Rupture of the diaphragm causes formation of a shock wave which propagates in the low- /11
pressure chamber in the negative x direction. In principle, the shock must remain weak so that the "thickness" of the expansion front will remain small. In the contrary case, the solution due to Mirels which is used for $\xi \leq 0$ is not strictly valid. In this problem it is the Ψ function which is used (the Φ function is not defined for $\xi < 0$), and so system (15) is used. Reference time is counted from diaphragm rupture: $t = 1$. The characteristic length is calculated for $L_0 = Q_0 t_0$, where Q_0 is the fluid velocity behind the shock, outside the boundary layer (i.e., that of the contact discontinuity at $\xi = 1$).

The results described agree with those of Mirels [4], [5], Bromberg [6], and Berstader and Allport [7] in the region $\xi \geq 1$, with those of Mirels [5] in the region $\xi \leq 0$, and agree with those obtained by Ban [8] and Ban and Kuerti [9] in the interaction zone $0 \leq \xi \leq 1$. These last authors were limited to the case of weak shock, and linearized system (15) with respect to the inverse of the shock intensity A. (It is expedient to define the intensity of a shock as the ratio of the shock velocity U_c to the fluid velocity behind the shock outside the boundary layer.)

5. PLAN AND GIVEN QUANTITIES OF THE STUDY

5.1 Type of Equations Treated

A simple model of the equations obtained for the problems considered appears to be:

$$\Phi \equiv \Phi_{,\eta\eta} - \xi(\eta - \xi)\Phi_{,\xi} = 0, \qquad \xi \geq 0. \tag{19}$$

For $\xi \geq 1$, equation (19) evolves in the direction of decreasing ξ.

For $0 \leq \xi \leq 1$, the direction of the evolution of the phenomena changes its direction when the line $\eta = \xi$ is crossed. It is thus clearly seen that the study must be conducted as follows:

1. Determination of the unknown function Φ (or Ψ) and T in the regions $\xi = 0$ (or $\xi \leq 0$) and $\xi \geq 1$, where the perturbations propagate in a single direction;

2. Study of the region $0 \leq \xi \leq 1$, the interaction zone, for which the perturbations propagate in the directions of increasing ξ and decreasing ξ at the same time, which requires consideration of Φ (or Ψ) and T at $\xi = 0$ and $\xi = 1$ as boundary conditions.

Note - Solution of this problem (similar in some ways to the separation problem) is possible only because the singular line $\eta = \xi$ is known. Only the Crocco transformation, which permits linearization of the convective terms, has this advantage. In the physical plane, the singular line $y(x,t)$ corresponding to $\eta = \xi$ is known only when u is given — i.e., when the problem has been solved.

5.2. External Flow

This is characterized by data on U and T_e.

Problem A:

$$U = 1; \quad \Phi = 0 \quad \text{at} \quad \eta = 1. \tag{20}$$

Problem B — Besides relations (20), it is necessary to determine T_e, which is obtained simply from T_w by the Rankine-Hugoniot relation. The physical data of the problem are, besides the wall temperature of the tube T_w, the shock velocity or its intensity A.

Problem C — The ratio of pressures in each chamber before rupture of the diaphragm and the temperature of the chambers, together with the shock-tube relationships, allow successive determination of:

a. the pressure at the contact discontinuity;
b. the velocity Q_0 of the contact discontinuity;

c. the reference temperature T_0;

d. the velocity $\overline{U}_c$ and the intensity A of the shock;

e. the velocity c_1 and the intensity B of the expansion front;

f. the temperature T_{e0} behind the contact discontinuity;

g. the temperature T_{e1} immediately behind the shock.

Temperature $T_e(\xi)$ is thus established, but has a discontinuity at $\xi = 1$. The point $\xi = \eta = 1$ is an isolated singularity since Φ ($\xi = 1$) and $T(\xi = 1)$ are continuous in the boundary layer. More precisely,

$$\lim_{\xi \to 1} T(\xi, \eta = 1) = T_{e0} < \lim_{\eta \to 1} T(\xi = 1, \eta) = T_{e1}. \tag{21}$$

The difference $T_{e1} - T_{e0}$ becomes larger as the shock is stronger.

5.3. Table of Chosen Values

Problem B — References: Q_0 = 36.8 m/s; T_0 = 4715°K

$$\begin{array}{llll} A = 9{,}95, & T_w = 62{,}18, & T_e = 64{,}89, \\ \chi = 2{,}2362\ (3), & \omega = 0{,}75, & Pr = 0{,}725. \end{array}$$

Problem C — 1. Weak shock

References: Q_0 = 36.8 m/s; T_0 = 4715°K

$$\begin{array}{llll} A = 9{,}95, & B = 9{,}33, & T_w = 62{,}18, & T_{e0} = 60{,}87, \\ T_{e1} = 64{,}89, & \chi = 2{,}32, & \omega = 0{,}7, & Pr = 0{,}725, \end{array}$$

2. Strong shock

References: Q_0 = 567.3 m/s; T_0 = 1121.4°K

$$\begin{array}{llll} A = 1{,}452, & B = 0{,}605, & T_w = 0{,}261, & T_{e0} = 0{,}117, \\ T_{e1} = 0{,}533, & \chi = 1{,}547, & \omega = 0{,}75, & Pr = 0{,}725, \end{array}$$

6. SOLUTION OUTSIDE THE INTERACTION ZONE

6.1 Region $\xi \geq 1$

This region corresponds to the time interval during which the effect of the leading edge does not make itself felt. Everything in Problems A and B occurs as if the plate were doubly infinite.

---

(3) The quantity $\chi = \sqrt{\frac{\overline{T}_w}{\overline{T}_0}} \frac{\overline{T}_0 + \overline{T}_s}{\overline{T}_w + \overline{T}_s}$ (where $\overline{T}_s = 116°K$), the Sutherland temperature of the gas), is the proportionality constant in the Chapman-Rubesin law, and is calculated by Sutherland's formula even if the Chapman-Rubesin law (ω = 1) is abandoned.

In Problem A, the solution is Rayleigh's solution $\Psi_R(\eta)$:

$$\left\{\begin{array}{l} \Psi_R \Psi_{R,\eta\eta_1} + \frac{1}{2} = 0, \\ \frac{\Psi_R \Psi_{R,\eta\eta}}{Pr} + \Psi_{R,\eta} T_{R,\eta}\left(\frac{1-Pr}{Pr}\right) + \frac{\Psi_R}{c_p} = 0. \end{array}\right| \tag{22}$$

Here, $\Phi(\xi = 1, \eta) = \Psi_R(\eta)$.

Problems B and C have a separated-variables solution studied by Mirels [10]:

$$\Psi(\xi, \eta) = \sqrt{\frac{A-1}{A-\xi}}\,\Psi_M(\eta); \qquad T(\xi, \eta) = T_M(\eta). \tag{23}$$

The functions Ψ_M and T_M satisfy[4]

$$\left\{\begin{array}{l} \Psi_M \Psi_{M,\eta\eta} + \frac{\rho\mu}{2}\left(\frac{A-1}{A-\eta}\right) = 0, \\ \frac{\Psi_M T_{M,\eta\eta}}{Pr} + \Psi_{M,\eta} T_{M,\eta}\left(\frac{1-Pr}{Pr}\right) + \frac{\Psi_M}{c_p} = 0. \end{array}\right| \tag{24}$$

After solution of system (30), one sets /14

$$\left\{\begin{array}{l} \Phi(\xi = 1, \eta) = \Psi(\xi = 1, \eta) = \Psi_M(\eta), \\ T(\xi = 1, \eta) = T_M(\eta). \end{array}\right| \tag{25}$$

6.2. Region $\xi \leq 0$.

For problems A and B, the equations are time-independent, since $\xi = 0$ corresponds to $t = \infty$. The solution is that of Blasius:

$$\left\{\begin{array}{l} \Phi_B \Phi_{B,\eta\eta_1} + \frac{\rho\mu\eta}{2}, \\ \frac{\Phi_B T_{B,\eta\eta}}{Pr} + \frac{\Phi_B}{c_p} + \Phi_{B,\eta} T_{B,\eta}\left(\frac{1-Pr}{Pr}\right) = 0. \end{array}\right| \tag{26}$$

In problem C, the equations do depend on t in the region $-B \leq \xi \leq 0$. According to Mirels [5] and Cohen [10], there is again separation of variables:

$$\Psi(\xi, \eta) = \sqrt{\frac{B}{B+\xi}}\,\Psi_c(\eta); \qquad T(\xi, \eta) = T_c(\eta). \tag{27}$$

which leads to solving

$$\left\{\begin{array}{l} \Psi_c \Psi_{c,\eta\eta} + \rho\mu\left(1 + \frac{\eta}{B}\right) = 0, \\ \frac{\Psi_c \Psi_{c,\eta\eta}}{Pr} + \frac{\Psi_c}{c_p} + \Psi_{c,\eta} T_{c,\eta}\left(\frac{1-Pr}{Pr}\right) = 0. \end{array}\right| \tag{28}$$

---

[4] System (24) reduces to system (22) when $A = \infty$ and $\rho\mu = 1$.

The solution having been reached, we set

$$\left.\begin{array}{l}\Phi(\xi=0)=\Phi_B(\eta)\\ T(\xi=0=T_B(\eta)\end{array}\right|\begin{array}{l}\text{or}\\ \text{or}\end{array}\left|\begin{array}{l}\Psi(\xi=0)=\Psi_c(\eta),\\ T(\xi=0)=T_c(\eta).\end{array}\right. \tag{29}$$

6.3. Method of Solution

All the equations considered are of the type

$$ff_{,\eta\eta}+\rho\mu\, h(\eta)=0; \tag{30a}$$

$$\frac{fg_{,\eta\eta}}{\mathrm{Pr}}+f_{,\eta}g_{,\eta}\left(\frac{1-\mathrm{Pr}}{\mathrm{Pr}}\right)+\frac{f}{c_p}=0, \tag{30b}$$

with the boundary conditions

$$\left\{\begin{array}{ll}f'=0, & g=g_w\\ f=0, & g=g_e\end{array}\right|\begin{array}{l}\text{at } \eta=0,\\ \text{at } \eta=1\end{array} \tag{31}$$

and the equation of state $\rho\mu=\mathcal{C}(g)$. Furthermore, the quantities $h(\eta)$, g_w, g_e, c_p, are given for the problem.

It may be noted immediately that a first integral of the energy is formulated in an obvious manner when Pr = 1, for any viscosity law $\rho\mu=\mathcal{C}(g)$.

Two integrations lead to Crocco's first integral

$$g=\frac{\eta}{c_p}(1-\eta)+(g_e-g_w)\eta+g_w. \tag{32}$$

If Pr = 1, equations (30a) and (30b) are decoupled. The temperature is first calculated by equation (32); this gives $\rho\mu=\mathcal{C}(g)$, and then equation (30a) is solved. If the quantity $\rho\mu$ is constant, equations (30a) and (30b) are again decoupled, but it is the friction coefficient f which is calculated first.

Finally, if Pr $\neq$ 1, and if the product $\rho\mu$ is effectively a function of g, there is no decoupling. One then iterates in the following manner: equation (32) gives a first series of values for the temperature g (η); the knowledge of the product $\rho\mu$ which results from this makes it possible to deduce a first iteration for the friction f. It is then possible to calculate a new value of the temperature g, and so on. The method converges rapidly, and it appears beneficial to over-relax strongly the iterations on f carried out after the system is made unsteady, in order to implement the calculation (Figure 4). The numerical treatment of each differential equation is performed at each iteration by a classical factorization method, on the basis of an implicit scheme.

7. TREATMENT OF THE INTERACTION ZONE

The following system is to be solved:

$$\left\{\begin{array}{l}\dfrac{\Phi^2\Phi_{,\eta\eta}}{\rho\mu}-\xi(\eta-\xi)\,\Phi_{,\xi}+\dfrac{\eta\Phi}{2}+\dfrac{\xi(\eta-\xi)}{\rho\mu}\,\Phi(\rho\mu)_{,\xi}=0,\\ \dfrac{\Phi^2 T_{,\eta\eta}}{\rho\mu}-\xi(\eta-\xi)\,T_{,\xi}+\dfrac{\Phi^2}{\rho\mu c_p}+\dfrac{\Phi\Phi_{,\eta}T_{,\eta}}{\rho\mu}\left(\dfrac{1-\mathrm{Pr}}{\mathrm{Pr}}\right)=0.\end{array}\right| \tag{33}$$

System (39) is first made unsteady by adding derivatives with respect to an artificial time τ to the second term. These terms are respectively $\Phi_{,\tau}$ and $T_{,\tau}$. The limits of Φ and T are then investigated for $\tau \to \infty$. The calculation is carried out after discrete formulation of the equations obtained, according to a scheme which is explicit and unconditionally stable. If the indices for discrete formulation with respect to τ, ξ, and η are respectively n, k, and p, and if the steps are $\Delta t, \Delta\xi, \Delta\eta$, the partial derivatives are approximated as follows:

$$\left\{\begin{array}{l}(\Phi_{,\eta})^{(n)}_{k,p}=\dfrac{\Phi^{(n)}_{k,p+1}-\Phi^{(n)}_{k,p}}{\Delta\eta},\\ (T_{,\eta})^{(n)}_{k,p}=\dfrac{T^{(n)}_{k,p+1}-T^{(n)}_{k,p-1}}{2\,\Delta\eta};\end{array}\right| \tag{34}$$

$$\left\{\begin{array}{l}(\Phi_{,\xi})^{(n)}_{k,p}=\dfrac{\Phi^{(n)}_{k+1,p}-\Phi^{(n)}_{k-1,p}}{2\,\Delta\xi},\\ (T_{,\xi})^{(n)}_{k,p}=\dfrac{T^{(n)}_{k+1,p}-T^{(n)}_{k-1,p}}{2\,\Delta\xi};\end{array}\right| \tag{35}$$

$$\left\{\begin{array}{l}(\Phi_{,\eta\eta})^{(n)}_{k,p}=\dfrac{\Phi^{(n)}_{n,p+1}-2\,\Phi^{(n+1)}_{k,p}+\Phi^{(n)}_{k,p-1}}{(\Delta\eta)^2},\\ (T_{,\eta\eta})^{(n)}_{k,p}=\dfrac{T^{(n)}_{k,p+1}-2\,T^{(n+1)}_{k,p}+T^{(n)}_{k,p-1}}{(\Delta\eta)^2}.\end{array}\right| \tag{36}$$

The off-centered scheme for $\Phi_{,\eta}$ (34) allows attenuation of the effect of the singularity at $\eta = 1$. The other centered schemes (34) and (35) give good accuracy. Finally, the discrete formulation (36) makes an explicit, unconditionally linearly stable scheme possible. It represents a classical harmonic analysis. If the condition $\dfrac{\Delta t}{(\Delta\eta)^2}$ = constant is satisfied, consistency with equations (33) is assured for $\tau = \infty$; $\Phi_{,\tau} = T_{,\tau} = 0$.

System (34) has been solved in this way for very dense nets: 25 points for $0 \leq \xi \leq 1$, and 50 points for $0 \leq \eta \leq 1$.

Solution is performed as for an elliptic system: i.e., by using the conditions at $\xi = 0$ and $\xi = 1$ previously determined in paragraph 6, together with the boundary conditions at $\eta = 0$ and $\eta = 1$. Iteration is performed based on

$$\left\{\begin{aligned}\Phi^{(1)}_{k,p} &= \Phi_{Bp} + \xi_k^2\left[\left(2\Phi_{Bp} - \frac{3}{2}\Phi_{Rp}\right)\xi_k + \frac{5}{2}\dot{\Phi}_{Rp} - 3\Phi_{Bp}\right],\\ T^{(1)}_{k,p} &= T_{Bp} + \xi_k^2[T_{Rp} - T_{Bp}].\end{aligned}\right| \tag{37}$$

These values for the functions $\Phi^{(1)}_{k,p}$ and $T^{(1)}_{k,p}$ are obtained by writing the continuity of the functions Φ and T at $\xi = 0$ and at $\xi = 1$, the continuity of the derivative Φ_ξ at $\xi = 1$, and its zero value at $\xi = 0$. When one iteration $\Phi^{(n)}$, $T^{(n)}$, $(\rho\mu)^{(n)}$ is known, a new temperature $T^{(n+1)}$ is calculated, from which we have

$$(\rho\mu)^* = \chi[T^{(n+1)}]^\omega, \tag{38}$$

then a new friction value Φ^*. Then one chooses

$$\Phi^{(n+1)} = \alpha\Phi^* + (1-\alpha)\,\Phi^{(n)} \tag{39}$$

and so on.

A test of the type /17

$$\operatorname{Sup}_{k,p}|\Phi^*_{k,p} - \Phi^{(n)}_{k,p}| < \varepsilon, \quad \text{where } \varepsilon = o[10^{-5}] \tag{40}$$

tells whether it is legitimate to stop the calculation. It has seemed necessary to make a slight under-relaxation for nets of large dimensions: $\alpha = 0.95$. This under-relaxation assures a regular decrease in the difference.

8. NUMERICAL RESULTS FOR PROBLEM A

1. It is clearly seen that the velocity profiles are sensitive to the fineness of the net chosen within the thickness of the boundary layer. Table I shows different values of the wall friction τ_p for the Rayleigh solutions at $\xi = 1$, and the Blasius solutions at $\xi = 0$.

TABLE I

	$\Delta\eta = 0{,}05$.	$\Delta\eta = 0{,}02$.	exact value
$\tau_p(\xi = 0)$.....	0,3296	0,3313	0,3319
$\tau_p(\xi = 1)$.....	0,5480	0,5579	0,5640

This small difference is due to the presence of a singularity of the form

$$\sigma = (1-\eta)\sqrt{-\operatorname{Log}(1-\eta)}$$

at the edge of the boundary layer. Its effect is very moderate, and justifies taking $\Phi = 0$ as the only condition at $\eta = 1$ (even though the nature of σ must require that $\Phi_{,\eta} = -\infty$).

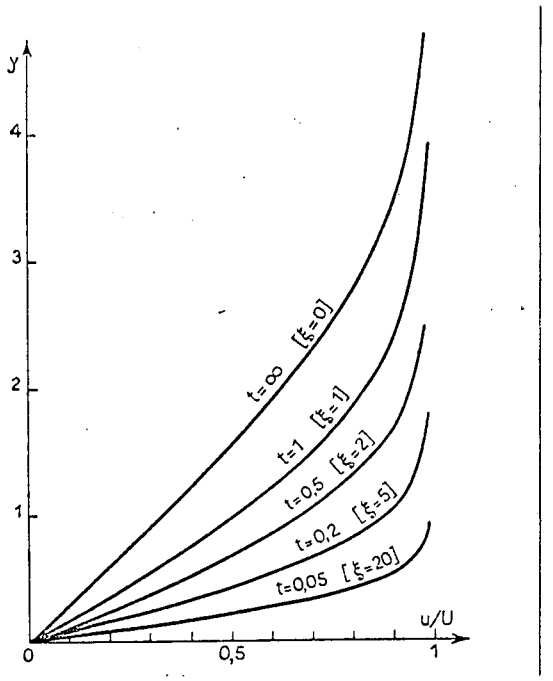

Figure 2 — Problem A.

Velocity profiles in the region $\xi \geq 1$ and at $\xi = 0$.

2. The solid line of Figure 1 shows the wall friction τ_p as a function of the ratio $\xi = \frac{x}{t}$ within the interaction zone (for $\xi > 1$, τ_p varies as $\sqrt{\xi}$). There is a small but nevertheless visible difference between two nets of different fineness. The results closest to those of Hall [2] and Lam and Crocco [3] correspond to the finest net.

3. Figures 2 and 3 show the variation of the velocity profiles with time at a given abscissa of the flat plate. These profiles agree well with those of Hall [2] and of Cheng and Elliott [11], except at the edge of the boundary layer, the slight difference being due to the fact that $\Phi_{,\eta}$ is poorly represented at $\eta = 1$. /19

9. NUMERICAL RESULTS IN THE CASE OF COUPLING

9.1. Iteration Conditions

When, thanks to case A, it has been demonstrated that the scheme converges in a satisfactory manner for a single equation, it is necessary to determine the relaxation coefficients which assure the most rapid convergence of the coupled system.

Figure 4 reveals that for Problem B (with a 10 x 20 net in the interaction

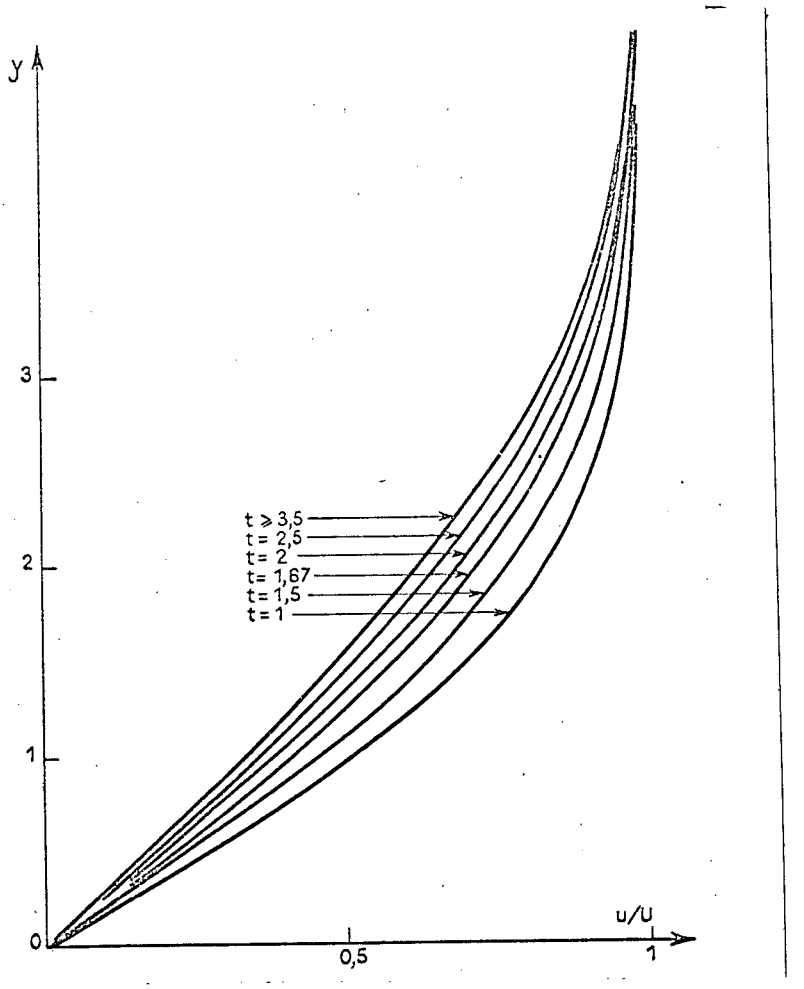

Figure 3 — Problem A

Velocity profiles in the interaction zone $0 \leq \xi \leq 1$.

zone), in the region $\xi \geq 1$ and at $\xi = 0$ — where a completely implicit scheme is used — it is advantageous to carry out a strong over-relaxation, which results in a large reduction in the number of iterations. On the other hand, if the relaxation factor is greater than 1 in the interaction zone, where the scheme is explicit, it easily destroys the convergence (for a 10 x 20 net, from $\alpha = 1.1$), with the result that it appears desirable to under-relax slightly, particularly for finer nets. /21

9.2. RESULTS FOR PROBLEM B

Figure 5 shows the variation of the velocity profiles with ξ for a weak shock. No new phenomenon appears in the incompressible case, except that obtaining the steady state requires a greater time delay ($t = 5$ instead of $t = 3.5$ in the

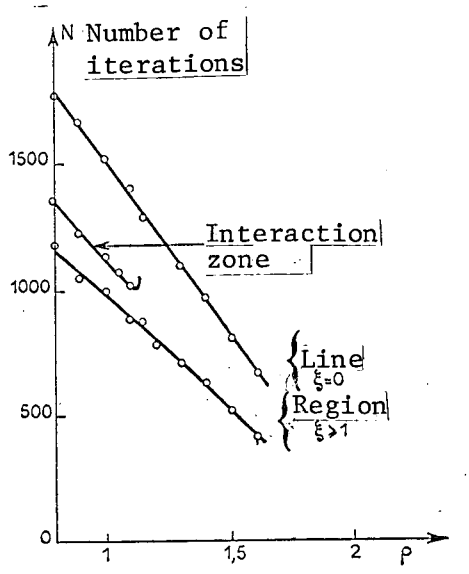

Figure 4 — Problem B

Influence of relaxation factor on convergence of the numerical schemes.

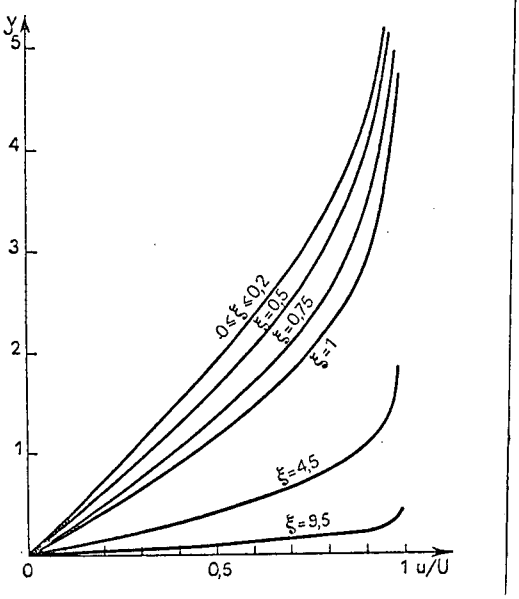

Figure 5 — Problem B

Behavior of velocity profiles.

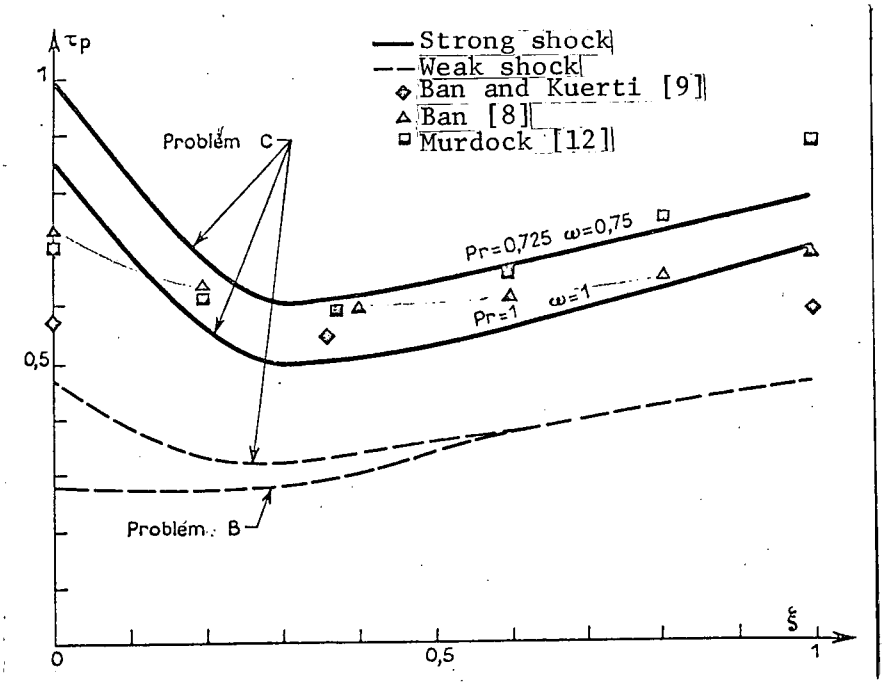

Figure 6 — Problems B and C

Wall friction in the interaction zone.

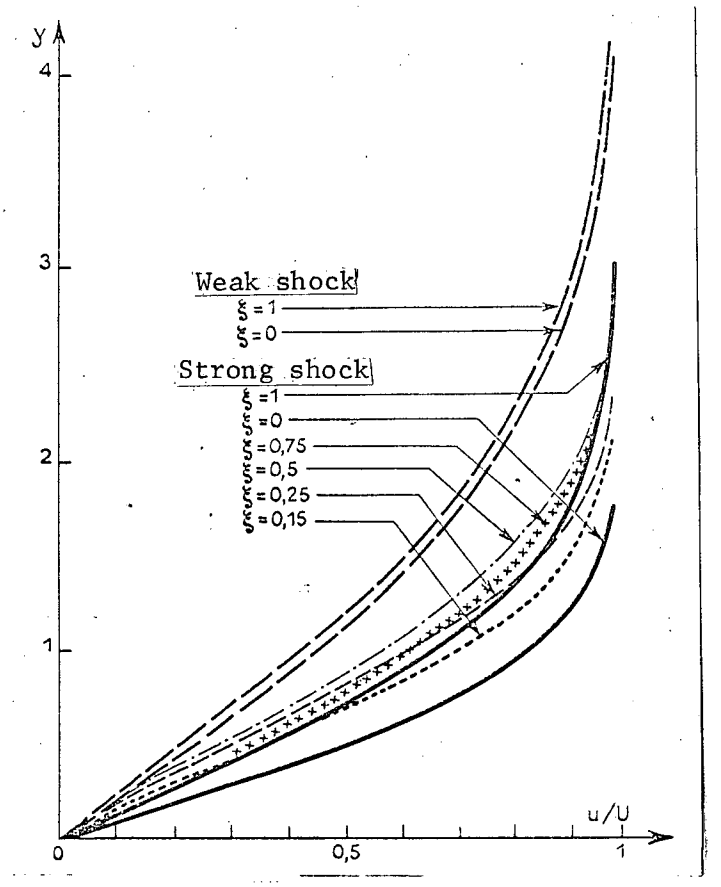

Figure 7 — Problem C

Behavior of velocity profiles in the interaction zone.

incompressible case). It is also clearly seen that the steady state is more slowly established as the shock is stronger.

The variation in wall friction τ_p (Figure 6) has been more closely studied /22 in the interaction zone, and compared with various results for the shock-tube problem. The difference between the conditions at $\xi = 0$ for Problems B and C is felt up to $\xi = 0.55$, indicating that the effect of upstream conditions is felt only after a certain time interval.

9.3. Problem C, the Shock Tube

Two cases have been considered. The weak shock corresponds to a low exterior fluid velocity, to a small temperature discontinuity at $\xi = 1$, and thus to moderate thermal perturbations in the boundary layer. The strong shock corresponds to a /23 much greater exterior fluid velocity, and to large temperature and velocity

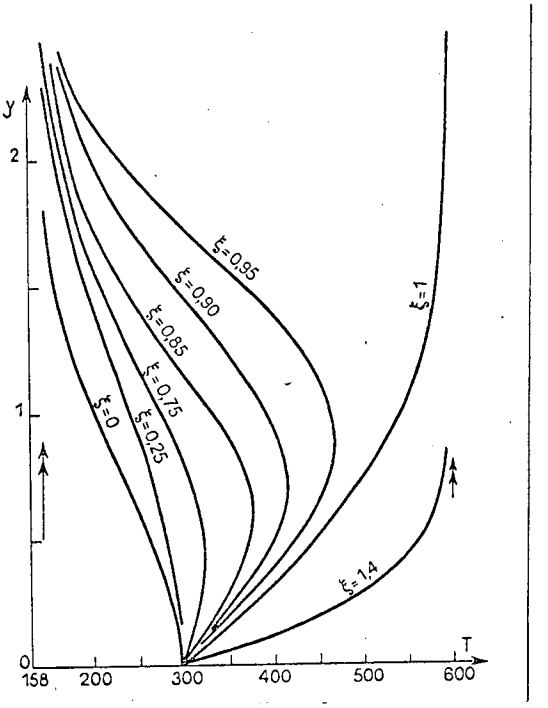

Figure 8 — Problem C

Behavior of the temperature profiles in a shock tube (strong shock).

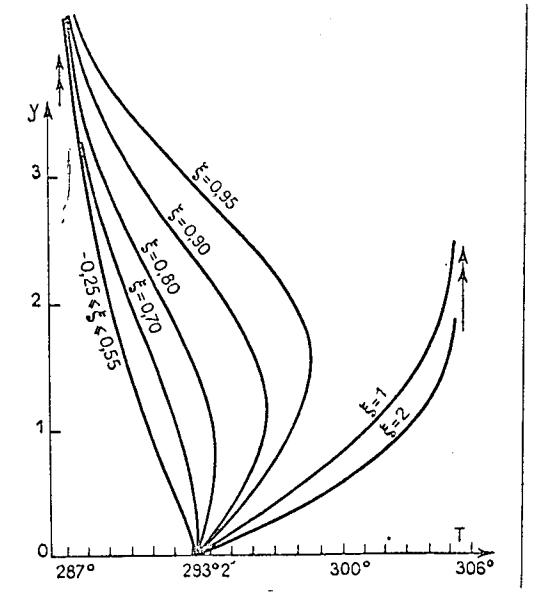

Figure 9 — Problem C

Behavior of temperature profiles in a shock tube (weak shock).

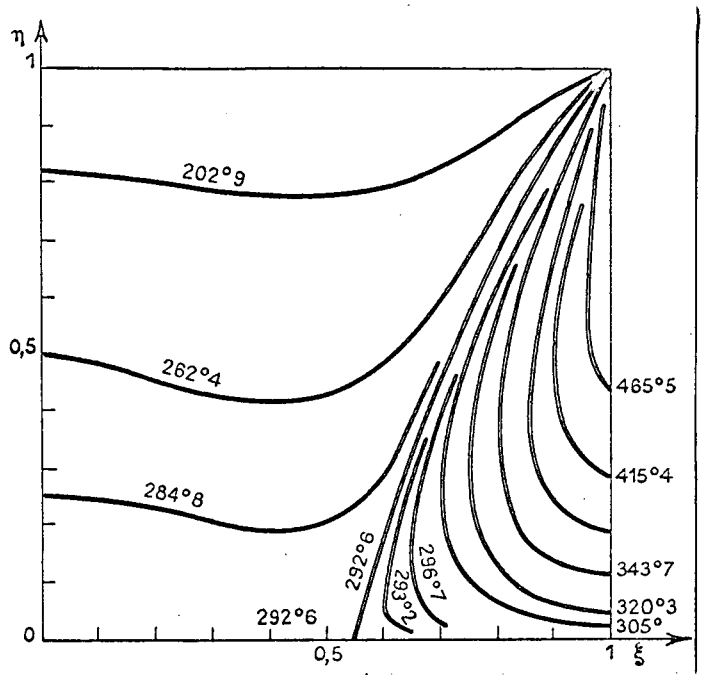

Figure 10 — Problem C

Isotherms in the interaction zone (strong shock, 20 x 40 net).

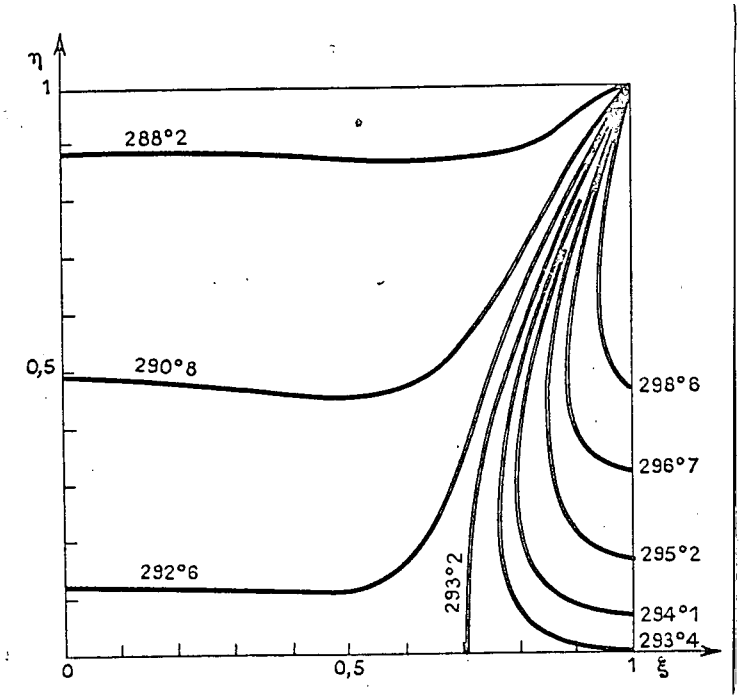

Figure 11 — Problem C

Isotherms in the interaction zone (weak shock, 20 x 40 net).

perturbations in the boundary layer. It is known, for example, that in this case, the thickness of the expansion front is far from negligible, so that a solution of a similar type, still used for $\xi \leq 0$, is not physically justified. Nevertheless, this has been retained in order to compare the present results with those of various authors, when possible, and also the better to concentrate attention on the interaction zone.

Figure 6 allows comparison of the values obtained by Murdock [12] and Ban [8] for wall friction with those obtained by the present method(5), for a strong shock with $\omega = 1$ and $Pr = 1$. The wall friction seems under-estimated with respect to that calculated by taking into account a more real physical situation ($\omega = 0.75$ and $Pr = 0.725$).

For a weak shock (only the case for $\omega = 0.75$ and $Pr = 0.725$ is represented), the situation is reversed, and the present data are clearly far removed from the /25
results of Ban and Kuerti [9], especially for $\xi = 1$.

Figure 7 shows that for a weak shock, the velocity profiles in the interaction zone are virtually superposed. This result is in good agreement with that of Ban and Kuerti [9]. In contrast, a crossing of the curves occurs for the strong shock; the function u/U increases out to a value of ξ of about 0.55, particularly near the plate (where inflection points seem to appear), then decreases to $\xi = 1$.

Figures 8 and 9 give the behavior of the temperature profiles in a shock tube, for a strong shock and for a weak one, respectively. The coordinate ξ represents the abscissa $\underline{x}$ where the temperature profile at time $t = 1$ is studied. Figures 10 and 11 show the temperature isotherms in the $\xi - \eta$ plane, for strong and weak shocks, respectively. The line of extension of the contact discontinuity in the /26
boundary layer is seen to be displaced toward smaller values of ξ as the intensity of the shock increases.

---

(5) In the following discussion, the accuracy ε required in the scheme is 0.5×10^{-4} for a strong shock, and 0.5×10^{-5} for a weak one. Finer requirements would entail prohibitive machine times.

10. CONCLUSION

It is evident from these studies that it is possible:

1. To deal with the problem of boundary layers on a flat plate, semi-infinite or not, induced by shock. This can be done in a more systematic and more general manner than by methods of the type of Lam and Crocco [3], Ban and Kuerti [9], or Murdock [12].

The method described here uses, as do the others, classical similarity properties and solutions of ordinary equations (Blasius, Rayleigh, and Mirels types). It justifies application of the Crocco transformation, despite the presence of a singularity at $\eta = 1$ resulting from the transformation from an infinite domain to a bounded one, and despite the possible contact discontinuity appearing at $\xi = \eta = 1$ in the shock-tube problem. One of the characteristics of the method is the treatment of the interaction zone with the aid of an explicit, unconditionally stable numerical schema.

2. To generalize the application of numerical treatment of equations with a pressure gradient, subject to a Crocco transformation, for any viscosity law and arbitrary Prandtl number. The obstacle then lies only in lack of knowledge of the exterior flow, and not in numerical problems resulting from ϕ - T coupling.

BIBLIOGRAPHY

1. Piquet, J. Numerical Solution of Certain Unsteady Incompressible Boundary Layers. La Rech. Aerosp., No. 1970-2, 1970, pp. 69 - 77.

2. Hall, M.G. The Boundary Layer Over an Impulsively Started Flat Plate. Proc. Roy. Soc., A, Vol. 310, 1969, pp. 401 - 414.

3. Lam, S.H. and L. Crocco. Shock - Induced Unsteady Laminar Compressible Boundary Layers on a Semi Infinite Flat Plate. Rept. No. 428, AFOSR TN 58 - 581, 1958.

4. Mirels, H. Laminar Boundary Layer behind a Shock Advancing into Stationary Fluid. NACA TN 3401, 1955.

5. Mirels, H. Boundary Layer behind Shock or Thin Expansion Wave Moving into Stationary Fluid. NACA TN 3712, 1956.

6. Bromberg, R. Use of the Shock Tube over an Impulsively Started Flat Plate. R.A.E., Techn. Rep. 68.088, 1956.

7. Berstader, D. and J. Allport. On the Laminar Boundary Layer Induced by a Traveling Shock Wave. Dept. of Phys. Techn. Rept. 11-22, Princeton University, 1956.

8. Ban, S.D. Interaction Region in the Boundary Layer of a Shock Tube. Case Inst. Rept. FTAS/TR 67-20; AFOSR Sci. Rept. 67-1286, 1967.

9. Ban, S.D. and G. Kuerti. The Interaction Region in the Boundary Layer of a Shock Tube. J. Fluid Mech., Vol. 38, Part 1, 1969, pp. 109 - 125.

10. Cohen, N. A Power-Series Solution for the Unsteady Laminar Boundary Layer Flow in an Expansion-Waive of Finite Width Moving Through a Gas Initially at Rest. NACA TN 3943, 1957.

11. Cheng, S.I. and D. Elliot. The Unsteady Laminar Boundary Layer on a Flat Plate. Trans. A.S.M.E., Vol. 79, 1957, pp. 725 - 733.

12. Murdock, H. A Solution of Shock-Induced Boundary Layer Problems by an Integral Method. Aerospace Rept. No. TR 01-58 (S 3816-63).2, 1968.

Translated for National Aeronautics and Space Administration under contract No. NASw 2035, by SCITRAN, P. O. Box 5456, Santa Barbara, California, 93108.